ISSN: 2249-7196
IJMRR/ Jan 2022/ Volume 12/Issue 1/-/1-10
Hazem M. El-Hageen / International Journal of Management Research & Review

Optical communication systems that use wide-band optical semiconductor amplifiers and high-speed signal processing

Hazem M. El-Hageen, Aadel M. Alatwi

Abstract: This work clarifies the analysis of the theoret- ical study of noise and transmission gain characteristics of semiconductor optical amplifiers (SOAs), which are relevant in the novel local area optical communication systems. We investigated the effects of noise on AlGaAs/ GaAs SOA transmission performance through the mea- surement of output power, optical gain, the optical signal-to-noise ratio, and noise figure. It was observed that noise has a dramatic effect on SOAs' operation transmission efficiency, and the performance of the amplifier structure may be limited. If the drive current and injection power at the SOA can be changed and its active region length modified, then the variation of gain, optical signal-to- noise ratio, and noise figure at the output of the structure can be obtained.

Keywords: device dimensions; gain bandwidth; noise figure; SOAs.

Introduction

Social and multimedia networks are designed to provide high data rates. These networks are used to carry big and real-time data such as video conferencing and video on demand [1, 2], where data losses are not allowed. Optical fiber cables constitute the most appropriate communica- tion link. When compared to radio channels or electrical cables, they have large bandwidth and provide low loss

levels [3-7]. It is clear that the demand for these types of networks and associated services will increase in the future; therefore, the importance of using optical fiber cables will increase. Their use will be expanded for ap- plications of fixed user locations. This calls for the development of optical fiber network components, espe- cially optical sources and detectors, to keep pace withincreasing network requirements [8, 9].

Modern studies have focused on attaining and enhancing high-capacity optical networks [10–12], with multiplexing techniques gaining the most attention in this regard. Wavelength division multiplexing technique de- pends on slicing the optical spectrum to multiple channels centered at different wavelengths [13–15], similar to the frequency division multiplexed technique in the radio broadcasting system. Wavelength division multiplexing systems include opto-couplers, optical amplifiers, wave- length multiplexers, demultiplexers, and tunable or fixed wavelength sources and detectors to cover the entire rangeof operating wavelengths [16, 17]. These components andother nonlinear devices in the link may cause inter-channel interference when optical pulses pass through them. Therefore, the various characteristic parameters of these components are preferred to be uniform in the operating wavelength range. The wavelength stability of sources andchannel spacing are among the most important parameters of interest [18] and are studied to optimize optical link per- formance in terms of inter-channel interference. The insta- bility of the source wavelength may drift it toward neighboring wavelength channels. Many stabilizing schemes of wavelengths have been proposed to avoid wavelength drift [19]. Most of these schemes adjust the source wavelength by comparing to a reference wavelength. Reducing channel spacing provides more channels in the spectral range but causes crosstalk; this requires narrow bandwidth filters, while the demultiplexers' resolution de- termines the channel spacing [20, 21]. In coherent receivers, the channel spacing can be smaller by two to four times more than in noncoherent receivers [22–24].

Because of the development of optical fiber communi-cation technology, optical fibers have become the dominantcarrier of the world's communication data, with a large ca-pacity reaching 100 Gb/s [25–31]. This capacity must be

accompanied by advances in signal amplification and pro-cessing [32-37]. Optical amplifiers are primarily used to boost light signals and in other applications, such as light switching and optical wavelength conversion [38–51]. Therefore, semiconductor optical amplifiers (SOAs) can be relied upon to make a big leap in the development of optical fiber networks.

coefficient, η_i is input coupling loss, I_D is the operating current, N_0 is carrier concentration, and τ_s is the sponta- neous recombination lifetime of the carriers. The amplifier

gain is usually specified in dB scale as the following expression [7-40]:

travelling-wave amplifier (TWA) has attracted consider- able attention. TWA is superior to the Fabry-Perot amplifier (FPA) in gain saturation, gain bandwidth, gain ripple, and noise figure. Figure 2 shows a TWA that worksas a single-pass amplifier. TWAs require a higher pump- ing rate to obtain a desired gain. Unlike Fabry-Perot amplifiers, TWAs have no mirror reflections, which can severely modulate the amplifier gain and considerably narrow the amplifier bandwidth [9]. To reduce facet reflection for TWA fabrication, the TWA has antireflection

Where G_s is the gain, h is Planck's constant, λ is signal

Where B_e is electrical bandwidth. Where the shot to spontaneous noise, the spontaneous-spontaneous noiseare given by the mathematical formula [1–40]:

coatings on the cleaved mirror facets and/or a tiltedwaveguide with respect to the facets.

The amplification of a signal with input power P_{in} in

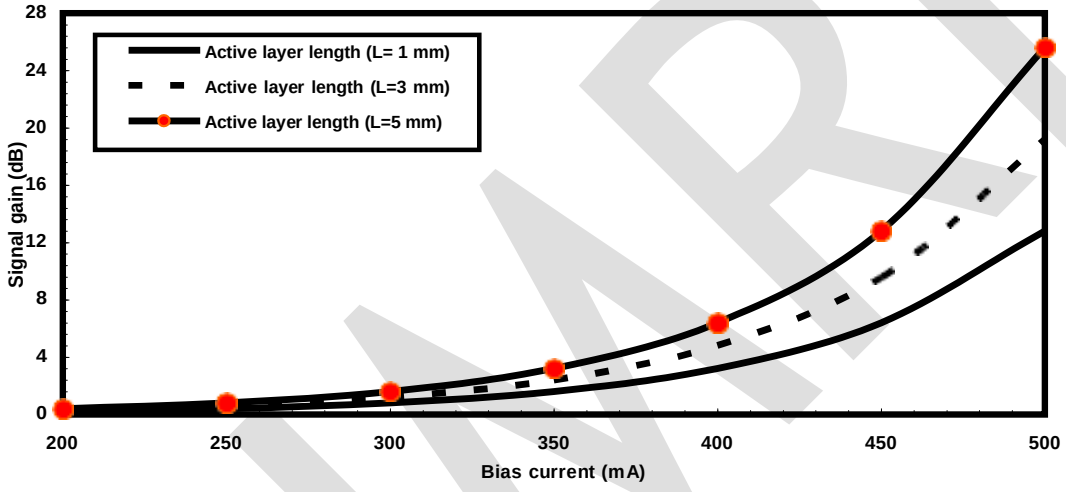

Figure 2: Signal gain variations in relation to the drive current for various active layer length of SOA.

I_D = 200 mA, 1.6 dB at I_D = 350 mA, and 12.8 dB at I_D = 500 mA for active amplifier layer length of 1 mm. As well as the amplifier signal gain is 0.3 dB at I_D = 200 mA,

The set of the parameters for $Al_xGa_{(1-x)}As$ material is recast with adjust as: $B_1 = 10.906\text{–}2.92\ x$, $B_2 = 0.97501$, $B_3 = b_3T^2$; $b_3 = (0.52886 - 0.735\ x/T_0)^2$, for $x < 0.36$. And $B_4 = b_4\ (0.93721 + 2.0857 \times 10^{-4}\ T)$; $b_4 = 0.002467(1.14\ x+1)$.
While for the parameters for GaAs material is recast as:

Table 1: Basic variables used in the study.

Variables	Definition	Values/units
P_{in}	Signal power	10 dBm
Λ	Signal wavelength	1550 nm
I_D	Drive current	200 mA-500 mA
L	Active layer length	1 mm-5 mm
W	Width of active layer	0.5 mm
D	Thickness of active layer	0.01 mm
Γ	Confinement factor	0.75
B_e	Electrical bandwidth	1 MHz
B_0	Optical bandwidth	1 GHz
n_{sp}	Spontaneous emission factor	$1.5 \times 10^{-16}\ m^3/s$
R_1	Input facet reflectivity	5×10^{-6}
R_2	Output facet reflectivity	5×10^{-6}
N_0	Carrier density at transparency	$1 \times 10^{24}\ m^{-3}$
τ_s	Recombination lifetime of the carriers	0.5 ps
g_m	Material gain	$3 \times 10^{6}\ m^{-1}$
g_0	Gain coefficient	$3 \times 10^{-20}\ m^2$
η_i	Input coupling loss	0.5 dB
K_0	Loss coefficient based carrier independent absorption	$6200\ m^{-1}$

$C_1 = 8.906$, $C_2 = 2.3501$, $C_3 = c_3T^2$, $c_3 = (0.25286/T_0)^2$, $C_4 = c_4$ (1.921 + 0.25710-4 T), and $c_4 = 0.03454$.

Numerical Simulation, Resultsand Analysis

The noise effect in the SOA device and its impact on the behavior of the structure over the operating variables. The signal power is 10 dBm at signal wavelength $\lambda = 1550$ nm. The drive current and the injection power can be studied at the SOA input and by modifying its active region length, the variation of gain, NF and OSNR at the output of the structure. The obtained results based on the clarified var- iables in Table 1, these parameters will be changed not only and 25.6 dB at $I_D = 500$ mA for active amplifier layer lengthof 5 mm. As both drive currents and active layer length increase, this results in the amplifier signal gain also increases.

Figure 3 shows the amplified spontaneous emission power in relation to the drive current for various active layer length of SOA. The amplified spontaneous emission power is 0.02 dBm at $I_D = 200$ mA, 0.16 dBm at $I_D = 350$ mA, and 1.28 dBm at $I_D = 500$ mA for active amplifier layer length of1 mm.

The amplified spontaneous emission power is 0.03 dBm at $I_D = 200$ mA, 0.24 dBm at $I_D = 350$ mA, and 1.92 dBm at $I_D = 500$ mA for active amplifier layer length of 3 mm.

The amplified spontaneous emission power is 0.04 dBm at $I_D = 200$ mA, 0.32 dBm $I_D = 350$ mA, and 2.56 dBm at $I_D = 500$ mA for active amplifier layer length of

5 mm. As both drive currents and active layer length in- crease, this results in the amplified spontaneous emission power also increases.

Figure 4 illustrates the Output (OSNR) variations with the drive current variations for various active layer length of SOA. The Output OSNR is 0.5 dB at a drive current of 200 mA, 1.5 dB at a drive current of 350 mA, and 6.5 dB at a drive current of 500 mA for active amplifier layer length of1 mm.

As well as the Output OSNR is 0.76 dB at a drive current of 200 mA, 2.34 dB at a drive current of 350 mA, and 8.3 at a drive current of 500 mA for active amplifier layer length of3 mm.

In addition to the Output OSNR is 1.75 dB at a drive current of 200 mA, 6.65 dB at a drive current of 350 mA, and 13.65 dB at a drive current of 500 mA for active amplifier

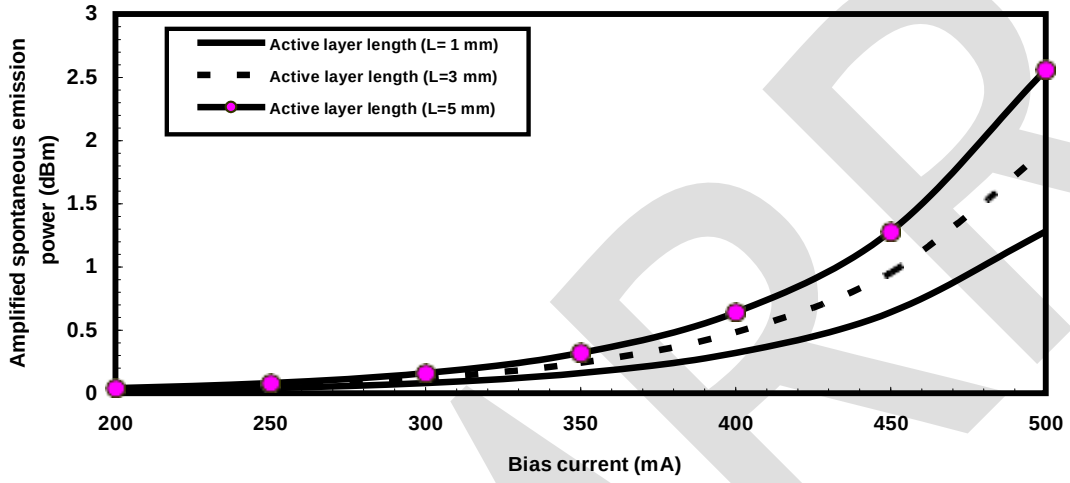

Figure 3: Amplified spontaneous emission power in relation to the drive current for various active layer length of SOA.

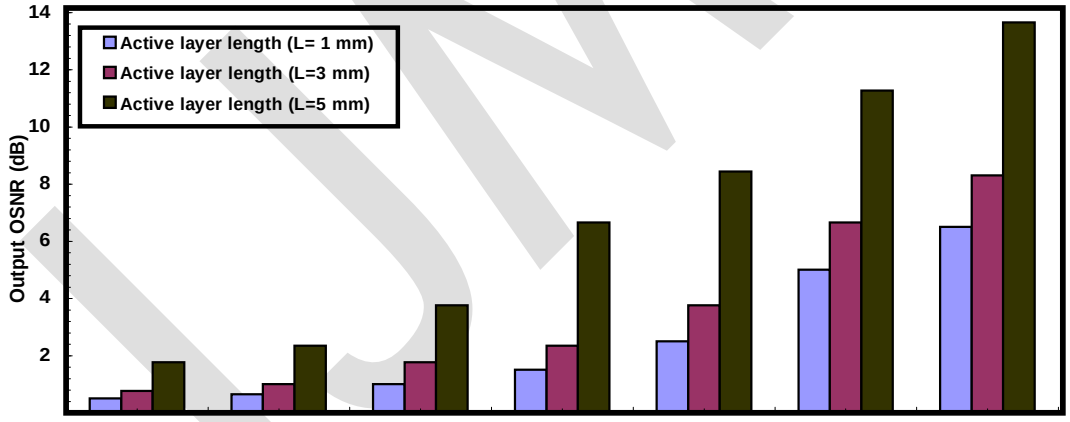

layer length of 5 mm. As both drive currents and active layer length increase, this results in the Output OSNR also increases.

As shown in Figure 5, the noise figure variations with the drive current variations for various active layer length of SOA. As both drive currents and active layer length in- crease, this results in the noise figure decreases.

The noise figure is 1.56 dB at a drive current of 200 mA, 1.2 dB at a drive current of 350 mA, and 0.9 dB at a drivecurrent of 500 mA for active amplifier layer length of 1 mm.As well as the noise figure is 1.4 dB at a drive current of 200 mA, 1.1 dB at a drive current of 350 mA, and 0.8 at adrive current of 500 mA for active amplifier layer length of 3 mm.

In addition to the noise, the figure is 1.3 dB at a drive current of 200 mA, 1 dB at a drive current of 350 mA, and 0.65 dB at a drive current of 500 mA for active amplifier layer length of 5 mm.

Figure 6 clarifies the signal gain variations with the ambient temperature variations for various drive currents based SOA. The signal gain increases with the increase of the amplifier drive currents with the adjustable of ambient temperature at 300 K. The signal gain is 12.8 dB at a tem- perature of 300 K, 2.4 dB at a temperature of 350 K, 0.2 dB ata temperature of 400 K for drive current of 200 mA.

The signal gain is 19.2 dB at a temperature of 300 K, 3.6 dB at a temperature of 350 K, 0.3 dB at a temperature of400 K for drive current of 350 mA. The signal gain is

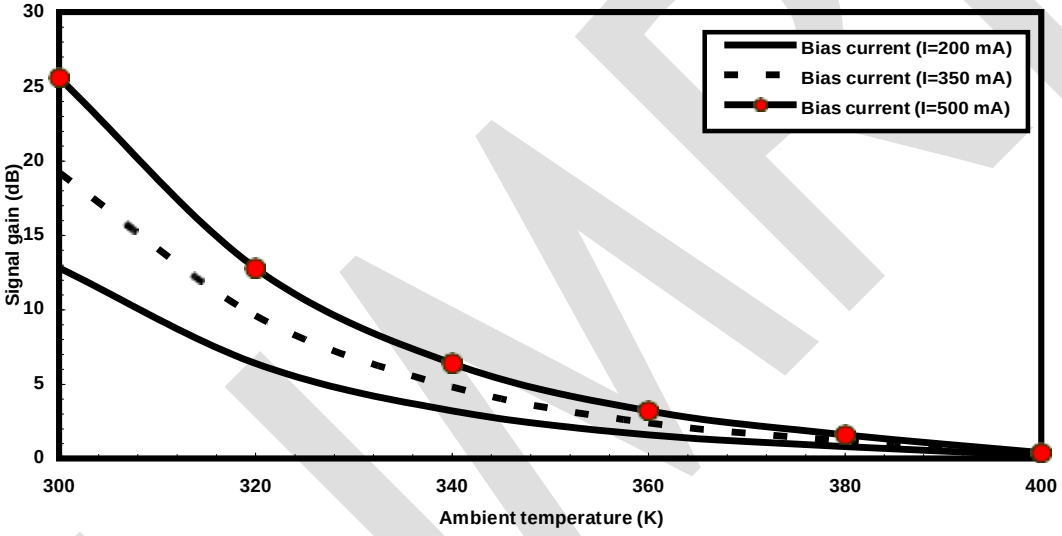

Figure 6: Signal gain variations with the ambient temperature variations for various drive currents based SOA.

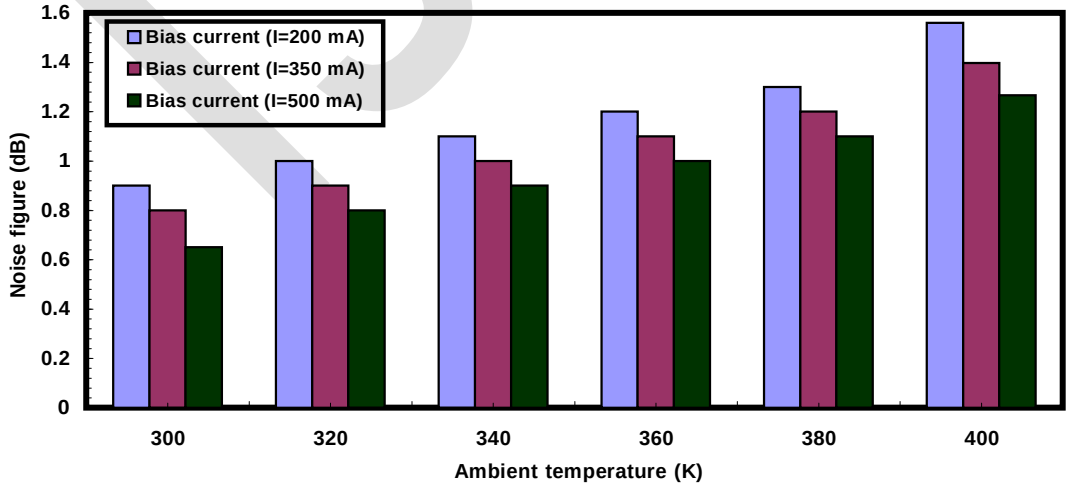

Figure 7: Variations of the noise figure with the ambient temperature variations for various drive currents based SOA.

25.6 dB at a temperature of 300 K, 5.324 dB at a temperature of 350 K, 0.4 dB at a temperature of 400 K for drive currentof

500 mA.

As shown in Figure 7, the variations of the noise figure with the ambient temperature variations for various drive currents based SOA. The noise figure decreases with the increase of the amplifier drive currents with the adjustable of ambient temperature at 300 K. The noise figure is

0.9 dB at a temperature of 300 K, 1.15 dB at a temperature of 350 K, 1.56 dB at a temperature of 400 K for drive current of 200 mA.

The noise figure is 0.8 dB at a temperature of 300 K,1 dB at a temperature of 350 K, 1.397 dB at a temperature of 400 K for drive current of 350 mA. The noise figure is

0.65 dB at a temperature of 300 K, 0.9 dB at a temperature of 350 K, 1.266 dB at a temperature of 400 K for drive current of 500 mA.

Conclusion

The signal gain and noise figure of the SOAs were investi- gated and discussed in detail under the variations of ambient temperatures and amplifier drive currents. The signal gain was enhanced and the noise figure was reduced under the control temperature 300 K and a drive current of 500 mA. The output light signal per noise ratio, signal gain, noise figure, and amplified spontaneous emission power were also adjusted and optimized under an active layer width of 5 mm, a temperature of 300 K and an amplifier drive current of 500 mA. This study demonstrates that traveling wave SOAs can be suitable for signal processing and wide bandwidth capability.

Author contribution: All the authors have accepted responsibility for the entire content of this submitted manuscript and approved submission.

Research funding: None declared.

Conflict of interest statement: The authors declare no conflicts of interest regarding this article.

References

Zhao M, Morthier G, Baets R. Analysis and optimization of intensity noise reduction in spectrum-sliced WDM systems using a saturated semiconductor optical amplifier. IEEE Photon. Technol. Lett. 2002;14:390–92.

Öhman F, Bishoff S, Tromborg B, Mørk J. Noise and regeneration in semiconductor waveguides with saturable gain and absorption. IEEE J. Quantum Electron. 2004;40:245–55.

Menif M, Mathlouthi W, Lemieux P, Rusch LA, Roy M. Error free transmission for incoherent broadband optical communications systems using incoherent-to-coherent wavelength conversion. IEEE J. Lightw. Technol. 2005;23:287–94.

Bernard J, Renaud M. Semiconductor optical amplifiers. SPIE's OE Magazine 2001;1:36–8.

Mork J, Nielsen ML, Berg TW. The dynamics of semiconductor optical amplifiers: modeling and applications. Opt Photon News 2003;14:42–8.

Kim H, Lee J. A gain-clamped SOA with distributed Bragg reflectors fabricated under both ends of active waveguide with different lengths. IEEE Photon Technol Lett 2004;16:999–1.

Björlin ES, Kimura T, Bowers JE. Carrier-confined vertical-cavity semiconductor optical amplifiers for higher gain and efficiency.IEEE J. Select. Top Quantum Electron. 2003;9:1374–385.

Said Y, Rezig H, Bouallegue A. Analysis of noise effects in long semiconductor optical amplifiers. The Open Opt J 2008;2:61–6.

Björlin ES, Geske J, Bowers JE. Optically preamplified receiver at 10 Gb/s using a vertical cavity SOA. Electron. Lett. 2001;37: 1474–5.

Chen X, Li J, Zhu P, Tang R, Chen Z, Yongqi. Fragmentation-aware routing and spectrum allocation scheme based on distribution of traffic bandwidth in elastic optical networks. IEEE/OSA J Opt Commu Netw 2015;7:1064–74.

Addis Mekonnen K, Tangdiongga E, Koonen AMJ. High-capacity dynamic indoor all-optical-wireless communication system backed up with millimeter-wave radio techniques. J LightwaveTechnol 2018;36:4460–7.

Nada B, Berceli T. Enhanced capacity of radio over fiber links using polarization multiplexed signal transmission. 20th Intern Conf Transp Opt Net 2018. https://doi.org/10.1109/icton.2018.8473732.

Öhman F, Bishoff S, Tromborg B, Mørk J. Noise and regeneration in semiconductor waveguides with saturable gain and absorption. IEEE J. Quantum Electron. 2004;40:245–55.

Zhao M, Morthier G, Baets R. Analysis and optimization of intensity noise reduction in spectrum-sliced WDM systems using a

saturated semiconductor optical amplifier. IEEE Photon.
Technol. Lett. 2002;14:390–2.
Menif M, Mathlouthi W, Lemieux P, Rusch LA, Roy M. Error free transmission for incoherent broadband optical communications systems using incoherent-to-coherent wavelength conversion. JLightw Technol. 2005;23:287–94.

Talli G, Adams MJ. Gain dynamics of semiconductor optical amplifiers and three-wavelength devices. IEEE J Quantum Electron. 2003;39:1305–13.

Tangdiongga E, Crijns JJJ, Spiekman LH, Van den Hoven GN, de Waardt H. Performance analysis of linear optical amplifiers in dynamic WDM systems. IEEE Photon. Technol. Lett. 2002;14:
1196–8.

Rieznik AA, Fragnito HL. Analytical solution for the dynamic behavior of erbium-doped fiber amplifiers with constant population inversion along the fiber. J Opt Soc Amer B Opt Phys.2004;21:1732–9.
Amiri IS, Zaki Rashed AN, Yupapin P. Interaction between optical sources and optical modulators for high-speed optical communication networks. J Opt Commu 2019 March 3. https://doi.org/10.1515/joc-2019-0041 [Epub ahead print].

Amiri IS, Zaki Rashed AN, Yupapin P. Effects of order super Gaussian pulses on the performance of high data rate optical fiber channel in the presence of self phase modulation. J Opt
Comm 2019. https://doi.org/10.1515/joc-2019-0039 [Epub
ahead print].

Amiri IS, Zaki Rashed AN, Yupapin P. Mathematical model analysis of dispersion and loss in photonic crystal fibers. J OptCommu 2019 April 5. https://doi.org/10.1515/joc-2019-0052 [Epub ahead print].

Amiri IS, Zaki Rashed AN, Yupapin P. Basic functions of fiber bragg grating effects on the optical fiber systems performance efficiency. J Opt Commu 2019 April 5. https://doi.org/10.1515/ joc-2019-0042 [Epub ahead print].

Amiri IS, Zaki Rashed AN, Mohammed El-NA, Aboelazm MB, Yupapin P. Nonlinear effects with semiconductor optical amplifiers. J Opt Commu 2019 April 12. https://doi.org/10.1515/
joc-2019-0053 [Epub ahead print].
Amiri IS, Zaki Rashed AN, Yupapin P. High-speed light sources inhigh-speed optical passive local area communication networks.
J Opt Comm 2019 April 20. https://doi.org/10.1515/joc-2019-0070 [Epub ahead print].

Connelly MJ, O'Dowd RF. Travelling-wave semiconductor optical amplifier detector noise characteristics. Proc Inst Elect Eng J 2015;142:23–8.

Chen Y-K, Chi S, Guo W-Y. High-flexibility configurations of amplifiedstar coupler for optical networks. J Opt Comm 1994;15:56–2.
Amiri IS, Zaki Rashed AN, Abd Elnaser AM, Ehab Salah E-D, Yupapin P. Spatial continuous wave laser and spatiotemporal vcsel for high-speed long haul optical wireless communication channels. J Opt Comm 2019 April 24. https://doi.org/10.1515/joc- 2019-0061 [Epub ahead print].

Amiri IS, Zaki Rashed AN, Yupapin P. Average power model of optical Raman amplifiers based on frequency spacing and amplifier section stage optimization. J Opt Comm 2019 May 4.https://doi.org/10.1515/joc-2019-0081 [Epub ahead print].
Amiri IS, Fatma Mohammed AMH, Zaki Rashed AN, Abd El-Naser AM. Temperature effects on characteristics and performance of near-infrared wide bandwidth for different avalanche photodiodes structures. Res Phy 2019;14:102399.
Amiri IS, Zaki Rashed AN. Simulative study of simple ring resonator-based brewster plate for power system operation stability. Indonesian J Elect Eng Comp Sci 2015;16:1070–6.

Amiri IS, Zaki Rashed AN. Different photonic crystal fibers configurations with the key solutions for the optimization of data rates transmission. J Opt Comm 2019 July 23. https://doi.org/10.1515/joc-2019-0100 [Epub ahead print].
Amiri IS, Zaki Rashed AN, Ramya KC, Vinoth Kumar K, Maheswar R. The physical parameters of EDFA and SOA optical amplifiers and bit sequence variations based optical pulse
generators impact on the performance of soliton transmission
systems. J Opt Comm 2015 July 31. https://doi.org/10.1515/joc-2019-0156 [Epub ahead print].
Amiri IS, Fatma Mohammed AMH, Zaki Rashed AN, Abd El-Naser AM. Optical networks performance optimization based on hybrid configurations of optical fiber amplifiers and optical
receivers. J Opt Comm 2019 July 31. https://doi.org/10.1515/joc-
2019-0153 [Epub ahead print].

Amiri IS, Zaki Rashed AN, Sarker K, Paul BK, Ahmed K. Chirped large mode area photonic crystal modal fibers and its resonance modes based on finite element technique. J Opt Comm 2019 July
23. https://doi.org/10.1515/joc-2019-0146 [Epub ahead print].
Amiri IS, Fatma Mohammed AMH, Zaki Rashed AN, Abd El-Naser AM. Comparative simulation of thermal noise effects for photodetectors on performance of long-haul DWDM optical networks. J Opt Comm 2019 August 10. https://doi.org/10.1515/ joc-2019-0152 [Epub ahead print].

Amiri IS, Zaki Rashed AN, Abd El-Naser AM, Mohamed BA. Singlewide band traveling wave semiconductor optical amplifiers for all optical bidirectional wavelength conversion. J Opt Comm 2019

August 10. https://doi.org/10.1515/joc-2019-0168 [Epub aheadprint].

Amiri IS, Zaki Rashed AN, Abd El-Naser AM, Walid Fawzy Z. Influence of loading, regeneration and recalling elements processes on the system behavior of all optical data bus line
system random access memory. J Opt Comm 2019 August 15.https://doi.org/10.1515/joc-2019-0163 [Epub ahead print].

Ramezani Z, Orouji AA, Aminbeidokhti A. A novel symmetric GaN MESFET by dual extra layers of Si3N4. Phy E: Low-Dimens Sys Nanostruct J 2015;70:135–40.

Orouji AA, Ramezani Z, Sheikholeslami SM. High-performance SOI MESFET with modified depletion region using a triple recessed gate for RF applications. Mat Sci Semicond Proc J 2015;
30:545–53.
Ramezani Z, Orouji AA. Investigation of veritcal graded channel doping in nanoscale fully-depleted SOI-MOSFET. Superlat Microstruc J 2016;98:359–70.

Anvarifard MK, Ramezani Z, Amiri IS. Proposal of an embedded nanogap biosensor by a graphene nanoribbon field effect transistor for biological samples detection. Phys Status Solidi (A)
2019 December 2019. https://doi.org/10.1002/pssa.201900879[Epub ahead print].

Anvarifard MK, Ramezani Z, Amiri IS, Nejad AM. A Nanoscale Modified band energy junctionless transistor with considerable progress on the electrical and frequency issue. Mat Sci Semicond
Proc J 2020;107:104849.
Ramezani Z, Orouji AA, Ghoreishi SA, Amiri IS. A Nano junctionless double-gate mosfet by using the charge plasma concept to improve short-channel effects and frequency characteristics. J Elect Mat 2019;48:7487–94.

Othman N, Tay KG, Mohd Shah NS, Talib R, Pakarzadeh H, Cholan NA. Saturation behavior of a one-pump fiber optical parametric amplifier in the presence of the fourth-order dispersion coefficient and dispersion fluctuation. Chinese Opt Lett 2019;17:110603.

Taghizadeh M, Tavassoly MK, Hatami M, Pakarzadeh H. One-pump fiber optical parametric amplifiers: from the pulsed to the continuous wave operation. Optical Engineering 2018;57:056103.

Pakarzadeh H, Golabi R, Peucheret C. Two-pump fiber optical parametric amplifiers: Beyond the 6-wave model. Opt Fiber Technol 2018;45:223–30.

Pakarzadeh H, Taghizadeh M, Hatami M. Designing a photonic crystal fiber for an ultra-broadband parametric amplification in telecommunication region. J Nonlin Opt Phy Mat 2016;25:
1650023.
Amiri IS, Zaki Rashed AN, Hala M, Kader A, Amr A, Awamry A, et al.Optical communication transmission systems improvement based on chromatic and polarization mode dispersion compensation simulation management. Opt J 2020;207:163853.
Samanta D, Sivaram M, Zaki Rashed AN, Boopathi CS. Amiri IS, Yupapin P. Distributed feedback laser (dfb) for signal power amplitude level improvement in long spectral band. J Opt Comm2020 April 2. https://doi.org/10.1515/joc-2019-0252 [Epub ahead print].

Amiri IS, Zaki Rashed AN, Yupapin P. Analytical model analysis ofreflection/transmission characteristics of long-period fiber bragg grating (lpfbg) by using coupled mode theory. J Opt Comm
2020 April 2. https://doi.org/10.1515/joc-2019-0187 [Epubahead print].
Amiri IS, Zaki Rashed AN, Rahman Z, Paul BK, Ahmed K. Conventional/phase shift dual drive Mach–Zehnder modulation measured type based radio over fiber systems. J Opt Comm 2020
April 14. https://doi.org/10.1515/joc-2019-0312 [Epub ahead print].